



university of
 groningen

faculty of science
and engineering

Regional Assessment of Geothermal Potential in Romania: a Volumetric Heat-in-Place Approach

Author:
Teodora NEAGA
(S5104629)

Supervisor:
prof. dr. Johannes MIOCIC
Second examiner :
prof. dr. Michael DEE

Bachelor's Thesis
To fulfill the requirements for the degree of
Bachelor of Science in Physics
at the University of Groningen

July 5, 2025

Contents

	Page
Abstract	3
Acknowledgements	4
1 Introduction	5
1.1 Geothermal Reservoir Properties	5
1.2 Current Status of Geothermal Energy in Romania	6
1.3 Aims and Objectives	9
1.4 Thesis Outline	9
2 Geological Setting	10
2.1 Transylvanian Basin	10
2.2 Pannonian Basin	11
2.3 Moesian Platform	13
3 Methodology	15
3.1 Geothermal Gradient	15
3.2 Recoverable Heat	15
3.2.1 Volume Estimation	15
3.2.2 Estimation of Reservoir Temperatures	16
3.2.3 Estimation of Recoverable Heat	16
3.2.4 Map Creation	16
4 Results and Discussion	18
4.1 Geothermal Gradient	18
4.2 Recoverable Heat	19
4.3 Future Outlooks	22
5 Conclusions	23
Bibliography	24
Appendices	30
A Raw Data	30
B Area and Volume Calculations	30
C Python Source Code	30

Abstract

Geothermal energy is a renewable energy source derived from the Earth's internal heat, and is considered a strong candidate for stable baseload energy, unlike other renewable sources that are limited by intermittency. In Romania, geothermal resources are limited to low-enthalpy uses such as balneology, greenhouse heating, and localized district heating. The national potential remains underutilized, with most developments concentrated in the western part of the country. The aim of this study was to investigate the geothermal resource potential of Romania, by combining geothermal gradient data with a volumetric heat-in-place approach, using geological cross sections from the three main sedimentary basins in the country: the Pannonian Basin, Transylvanian Basin, and Moesian Platform. The results show that geothermal gradients vary significantly across the country, ranging between 16 and 50 °C · km⁻¹, with the highest values recorded in the Pannonian Basin. Their distribution is broadly consistent with current applications, but reveal untapped potential in the Moesian Platform and Transylvanian Basin. The total recoverable heat was estimated at approximately 634 EJ over a surface area of 5080 km². The calculated technical potential is around 0.016 EJ per year, which represents around 4% of Romania's annual heating and cooling demand. The main limitation of this study was the lack of publicly available data, which restricted the analysis to around 2% of Romania's surface area, and required the use of generalized reservoir properties. Despite these limitations, the findings indicate substantial unexploited geothermal potential. Future research should expand the geographic scope of the study and incorporate higher-resolution subsurface data to improve the accuracy of the estimates and better assess the ability of geothermal energy to help reduce fossil fuel dependency.

Acknowledgments

First and foremost, I would like to thank my supervisor, Johannes, for his guidance, support, and admirable patience in answering every single one of my questions, no matter how many there were. I would also like to express my gratitude to Professor Codruța Bendea from the University of Oradea for providing insights regarding the current use of geothermal energy in Romania. Special thanks to Cătălin for helping with the Python code used in the analysis. Last but not least, I would like to thank myself for powering through the data gaps, the deadline stress, and QGIS crashing precisely when it should not.

1 Introduction

The use of geothermal energy can be traced back thousands of years, when early civilizations used hot springs for bathing, cooking, and healing purposes [1]. Today, geothermal energy is considered a renewable energy source, as it draws on the Earth's internal heat, which is mainly produced by the natural decay of radioactive isotopes, such as uranium, thorium, and potassium, as well as from the residual heat from planet formation [2, 3]. Given the extremely long half-lives of these isotopes, especially that of thorium-232, which is 14.1 billion years [4], the internal heat of the Earth can be regarded as constant. This makes geothermal energy a great candidate for stable and reliable baseload energy, in contrast to other renewable sources that are limited by intermittency [5].

To access this energy, geothermal systems rely on the circulation of water through the subsurface [1]. Surface water infiltrates downward through porous and permeable rocks, absorbs the heat, and is then extracted to the surface through wells drilled into reservoirs [6, 7]. Depending on the temperature of the resource, geothermal energy can be used either for direct applications, such as space and district heating, when temperatures are below 150 °C (low enthalpy), or for electricity generation, when they exceed that threshold (high enthalpy) [8].

In both cases, the extracted fluid, after the heat is removed, is generally reinjected into the reservoir. This is done to ensure the long-term stability of the system and to minimize the environmental impact of the surface discharge of geothermal fluids [9, 10]. It also helps preserve the pressure gradient, which drives fluid circulation and maintains the flow to the production wells, and the temperature of the reservoir [9, 11]. However, if the reinjection well is placed too close to the production well, the reinjected fluid, which is considerably cooler, will not have enough time to reheat, which could lead to thermal breakthrough [12]. This would further lead to a temperature reduction in the production well, and subsequently a reduction of the efficiency and life-time of the reservoir [13].

1.1 Geothermal Reservoir Properties

For a geothermal reservoir to be considered ideal for energy use, several conditions must be met. Firstly, a high geothermal gradient, which is the rate at which temperature increases with depth, is preferred, as it allows sufficiently high temperatures to be reached at shallower depths, thereby reducing drilling costs [14, 15]. Although the global average is below $30^{\circ}\text{C} \cdot \text{km}^{-1}$, this value can rise significantly in regions affected by geological anomalies [14]. These include areas with recent or ongoing volcanic activity, areas with fault systems, or regions where the Earth's crust is thinner [14]. These allow the heat from the mantle to reach shallower depths more efficiently, and thereby create favorable conditions for geothermal development [14].

Additionally, reservoir rocks must exhibit both high porosity, which allows large amounts of hot water to accumulate in the pore space, and high permeability, which enables this water to circulate through the subsurface [16]. These conditions are generally met in porous formations such as sandstone, limestone, and fractured volcanic rocks [12, 16].

For low-porosity rocks, such as granite, a critical factor is the presence of natural fractures, which are networks of cracks and faults within the rocks that significantly enhance permeability by providing preferential flow paths for the geothermal fluid, commonly encountered in

either liquid or vapor form [16, 17, 18]. In cases where high temperatures are present but the rock layers showcase low permeability and lack natural fractures, artificial fracturing can be used to improve fluid flow and make the reservoir suitable for geothermal production [16, 19]. This technique, however, can lead to induced seismicity, which poses social and environmental concerns [20].

To ensure that both the geothermal fluid and its heat remain contained, the reservoir must be capped by layers of impermeable rocks, such as clay or shale, that act as seals [21]. These confining layers prevent the upward migration of hot water while also creating a protective barrier such that the groundwater is not contaminated by the geothermal fluid [22], which often contains dissolved organic and inorganic compounds that could degrade the quality of surrounding clean water [23, 24].

1.2 Current Status of Geothermal Energy in Romania

Romania has considerable geothermal potential, in the form of low-enthalpy resources, which typically range between 40°C and 120°C [25]. In the year 2015, around 100 wells were operational in that temperature range, 40 of them being used exclusively for balneology and bathing [26]. A map of the main geothermal reservoirs is presented in Figure 1.

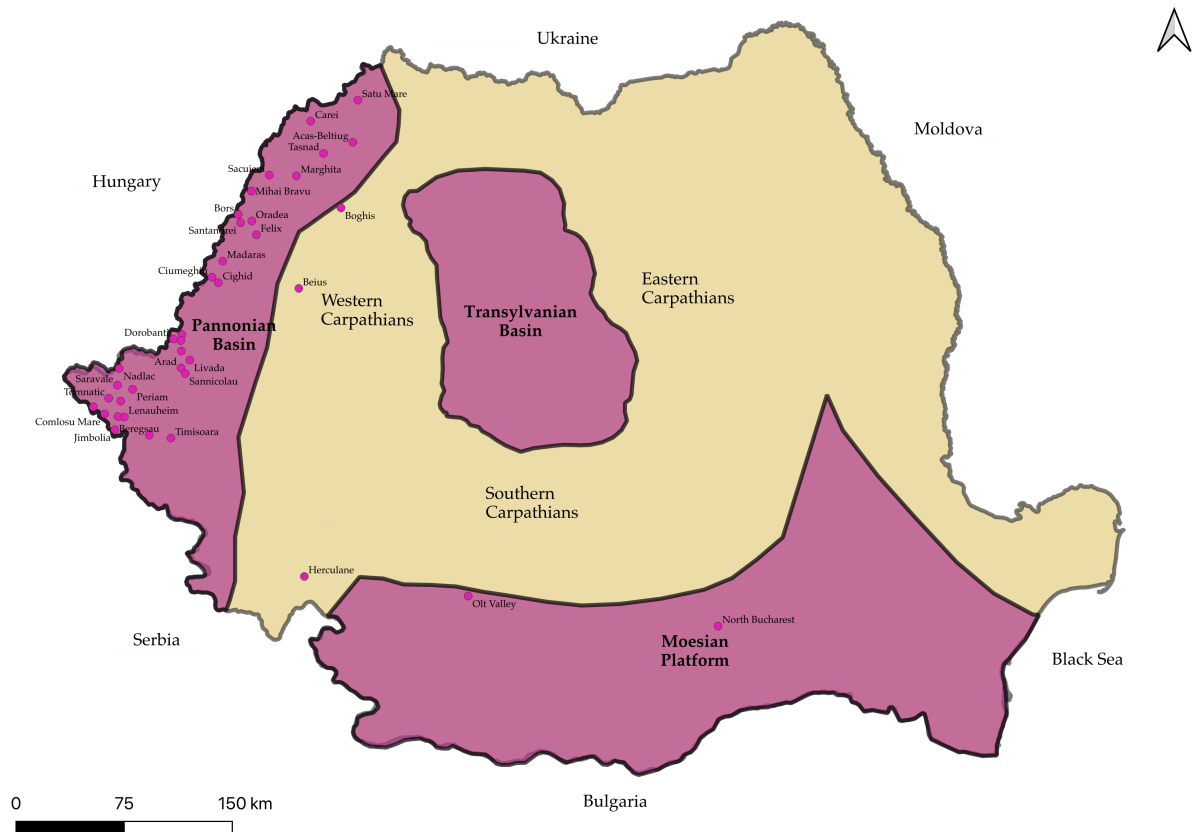


Figure 1: Location of the Pannonian Basin, the Transylvanian Basin, and the Moesian Platform. The major mountain ranges are labeled to indicate regional structural boundaries. The dots indicate the localities using geothermal systems (an overview of the main utilizations and parameters per locality can be found in Table 2).

The geothermal reservoirs are mainly located within two distinct geological settings. The first includes porous and permeable sedimentary formations, such as sandstones and gritstones, typically found in the Western Plain and the Olt Valley [26, 27]. The second consists of fractured carbonate formations, which are characteristic of areas such as Oradea, Bors, Beius, and North Bucharest [26, 27]. Table 1 depicts site-specific characteristics of the main geothermal systems in Romania.

Table 1: *Main parameters of the most important geothermal systems in Romania, as of 2010, obtained from [27].*

Parameter	Unit	Oradea	Bors	Beius	Western Plain	Olt Valley	N Bucharest
Type of reservoir	–	carbonate	carbonate	carbonate	sandstone	gritstone	carbonate
Area	km ²	75	12	47	2,500	10	350
Depth	km	2.2 – 3.2	2.4 – 2.8	2.4 – 2.8	0.8 – 2.39	2.7 – 3.25	2.0 – 3.2
Drilled wells	(total)	14	6	2	88	4	17
Active wells	–	12	0	2	39	2	1
Well head temp.	°C	70 – 105	120	84	50 – 90	70 – 95	51 – 84
Temperature gradient	°C/100	3.5 – 4.3	4.5 – 5.0	3.3	3.75 – 4.15	3.0 – 3.5	2.3 – 2.6
Total Dissolved Solids	g/l	0.8 – 1.4	12 – 14	0.46	2 – 6	15.7	2.2
Gas-to-Water Ratio	Nm ³ /m ³	0.05	5.0 – 6.5	–	0.6 – 2.1	1 – 2	0.1
Type of production	–	Artesian	Artesian	Pumping	Art. + Pumping	Artesian	Pumping
Flow rate	l/s	4 – 20	10 – 15	13 – 44	4 – 12	8.5 – 22	22 – 28
Operations	–	11	2	1	18	3	1
Annual savings	toe	9700	3200	1000	18500	3500	1900
Total installed power	MW _t	58	25	10	30	12.5	35
Exploitable reserves (20 years)	MW/day	570	110	52	4700	300	840

The existing wells provide a total installed capacity of 480 MWt (at a reference temperature of 25°C), with only 200 MWt used. This results in an annual utilization of around 400 GWh [26], or approximately 0.16% of the country's annual energy demand [28]. These resources are predominantly used for various forms of direct heat utilization, such as space and district heating, domestic hot water supply, greenhouse heating, health and recreational bathing, or industrial processes [26, 29]. A detailed overview of geothermal systems and their primary utilization per locality is presented in Table 2.

Although Romania has significant geothermal resources, the use of geothermal energy remains limited, being concentrated mainly in the western part of the country. In recent years, however, a growing number of municipalities have begun exploring or expanding the use of geothermal energy for urban and semi-urban heating purposes [30, 31, 32, 33]. Despite these successful examples, which highlight a substantial, untapped potential, the national picture remains one of underutilization [34]. Most geothermal energy applications in Romania are still directed toward individual facilities, such as spas, greenhouses, and isolated buildings, with limited integration into large scale systems, such as district heating networks, which could contribute to meeting the national heating demand and reduce the reliance on fossil fuels. Compared to other renewable technologies, such as biomass or solar energy, the expansion of geothermal heating has been slower, primarily due to data gaps, financing challenges, and insufficient technical modernization [34].

Table 2: Utilization of geothermal energy for direct heat as of 31 December 2014, obtained from [35]. *H* = Space heating and district heating (other than heat pumps), *I* = Industrial process heat, *B* = Bathing and swimming (including balneology), *G* = Greenhouse and soil heating, *F* = Fish and animal farming, *D* = drying agricultural products. *Wells above 50° wellhead temperature, without Exploration Permit (NAMR License), in stand-by. **Maximum annual average flow rate approved by the NAMR License.

Locality	Utilization	Flow Rate [kg/s]	Inlet Temperature [°C]	Outlet Temperature [°C]	Capacity [MWt]	Average Flow [kg/s]	Energy [TJ/yr]	Capacity Factor
Satu Mare	HB	22.9	65	30	3.36	7.00	32.30	0.31
Carei	B	10.3	45	30	0.65	3.00	5.90	0.29
Acas-Beltiug	B	31	68	30	4.93	0.25	3.40	0.02
Tasnad	BH	17	70	25	3.20	0.17	26.23	0.26
Sacuieni	HDBG	58	80	25	13.36	8.20	30.08	0.07
Marghita	HDB	26	65	25	4.35	5.00	14.57	0.11
Boghis	BH	12	45	25	1.00	5.00	7.23	0.23
*Mihai Bravu	GF	6	65	25	1.00	0.00	0.00	0.00
Sannicoau de Munte	B	5	65	25	0.84	0.17	0.74	0.03
Bors	D	25	120	40	8.37	3.00	6.64	0.03
**Oradea	HDB	90	87	30	21.48	65.00	345.76	0.51
Livada	DG	10	88	30	2.43	9.00	2.26	0.03
Felix	BH	140	45	25	11.72	95.00	250.61	0.68
Madaras	BH	7	46	25	0.62	0.16	1.19	0.06
Ciumeghiu	G	12	92	35	2.86	0.00	0.00	0.00
Cighid	HB	10	72	25	1.97	0.37	2.75	0.04
Beius	HDB	120	84	30	27.13	15.48	158.46	0.19
Santandrei	F	25	79	35	4.61	2.00	9.70	0.07
Macea	HGB	12	57	30	1.36	10.00	19.53	0.46
Curtici	HGB	16	57	30	1.81	13.00	25.39	0.45
Dorobanti	GB	12	57	30	1.36	5.00	9.77	0.23
*Sofronea	HB	6	50	30	0.50	0.00	0.00	0.00
Arad	B	12	40	25	0.75	7.00	7.60	0.32
Nadlac	IDB	10	75	35	1.67	5.00	14.47	0.27
Sannicolau	IDB	15	78	35	2.70	5.00	15.55	0.18
Saravale	HB	8	75	35	1.34	0.00	0.00	0.00
Tomnatic	GB	45	78	35	8.10	0.00	0.00	0.00
Lovrin	DGB	8	78	35	1.44	5.20	30.02	0.66
*Periam	HB	10	70	35	1.47	0.00	0.00	0.00
Jimbolia	IDBG	8	78	35	1.44	1.00	5.67	0.12
*Teremia	GHB	10	80	35	1.88	0.00	0.00	0.00
*Lenaueim	HBG	8	80	35	1.51	0.00	0.00	0.00
*Comlosu Mare	HB	5	70	35	0.73	0.00	0.00	0.00
*Grabat	GB	10	80	35	1.88	0.00	0.00	0.00
*Beregsau	GB	6	72	35	0.93	0.00	0.00	0.00
Timisoara	DB	10	50	35	0.63	1.00	1.98	0.10
Herculane	B	75	52	25	8.48	50.00	148.00	0.55
Olt Valley	DB	45	92	35	10.74	19.00	142.82	0.42
North Bucharest	HB	242	75	35	40.53	2.00	0.06	0.00

1.3 Aims and Objectives

The research question investigated throughout this study is "What is the geothermal potential of Romania?". The analysis is based on geothermal gradient mapping and estimates of the total heat that could theoretically be extracted from reservoir rocks. A volumetric heat-in-place approach is used, focusing on the country's main sedimentary basins, which appear to have favorable conditions for geothermal reservoirs. Existing research in this field is limited, as most studies focus solely on currently exploited wells. The main motivation behind the investigation lies in the fact that available studies briefly mention the geothermal potential across Romania, but do so without presenting the underlying methodology, which makes it difficult to verify or build upon their conclusions.

1.4 Thesis Outline

In the remainder of the thesis, the geological setting of the northeastern part of the Pannonian Basin, the Transylvanian Basin and the Moesian Platform is provided in Section 2. Section 3 outlines the methodology used to generate the geothermal gradient map and to compute the recoverable heat estimates. Section 4 presents the main findings and their interpretation, a discussion of the main limitations, and suggestions for improvement. Lastly, Section 5 provides a summary of the main findings and future directions.

2 Geological Setting

Sedimentary basins are areas of the Earth's crust that contain thick accumulations of sedimentary rocks [36]. These successions typically consist of alternating permeable and impermeable layers, which facilitate the formation of reservoir-seal systems [37]. Their widespread distribution, large size, and frequent proximity to human settlements make them highly accessible for geothermal development [38]. Furthermore, sedimentary basins host a significant amount of thermal energy, as a result of heat conducted from the inner crust and retained during the lithification of their sedimentary sequences [39]. While these basins share similar features, they differ in terms of geological age, lithology, and stratigraphic architecture [40]. These differences reflect distinct tectonic settings and sedimentation histories, which are typically classified according to the geological time scale [41].

In the following subsections, the geological setting of the three sedimentary basins selected for this study will be presented. This includes information about their structural layout, stratigraphy, and lithology, which represent key factors in evaluating the resource potential of each basin.

2.1 Transylvanian Basin

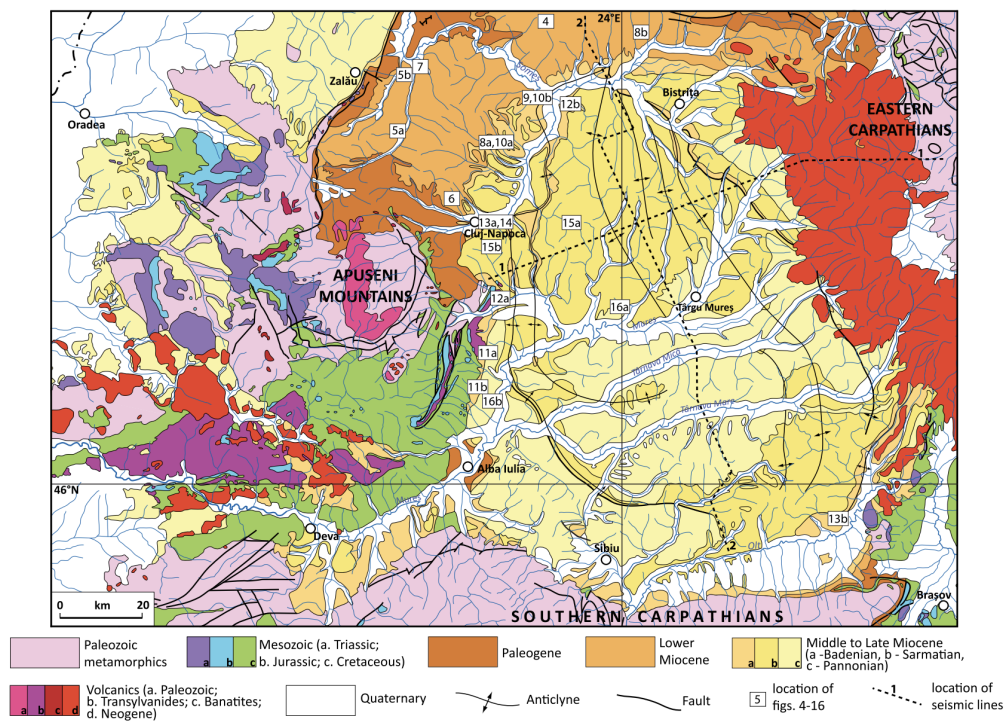


Figure 2: Location and general geology of the Transylvanian Basin, obtained from [42].

The Transylvanian Basin (Figure 2) is a sedimentary back-arc basin situated between the Apuseni Mountains (in the Western Carpathians) and the Eastern and Southern Carpathians [42]. The Carpathians, which are related to the Alpine orogen, were created during the convergence between the African and European plates [43]. The basement of the Transylvanian Basin began forming from the Middle Cretaceous, as a consequence of the tectonic collisions

in the intra-Carpathian region [42]. Covering an area of around 20000 km², the Transylvanian Basin represents the primary gas-producing region in Romania and in Central Eastern Europe [44],[45]. The sedimentary fill of the basin, built upon the Middle Cretaceous basement, is between 5 and 8 km thick and comprises Upper Cretaceous to Upper Miocene deposits, with gas being produced between the Middle to Upper Miocene sequence [44].

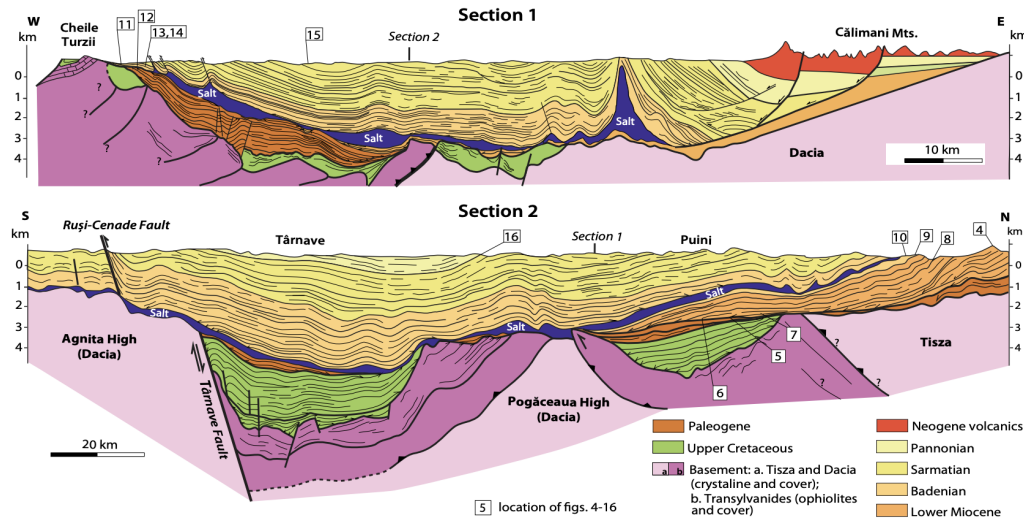


Figure 3: Regional sections depicting the overall basin architecture, obtained from [42]. Their approximate location can be seen in Figure 2.

The stratigraphy of the basin is illustrated in the cross-sections presented in Figure 3. The lower level of the basin contains Upper Cretaceous sediments, which are mostly comprised of clays, marls and sandstones, followed by Paleogene deposits [46]. The Lower Miocene deposits consist of sandstone, mudstone, and turbidites [42]. The Badenian sedimentation begins with a tuff and conglomerate formation, overlapped by a salt formation that creates diapirs, and ends with sands and marls [44]. The Sarmatian deposits comprise mostly sands and marls, with few conglomerates in the eastern part, while the Pannonian deposits conclude the sedimentation of the basin with sands and marls [44].

Although magmatic activity took place during Late-Cretaceous to Neogene near the basin, it was restricted to its margins. The basin shows relatively low heat flow, decreasing from around 60 mW · m⁻² in the north, to 40 mW · m⁻² in the south, likely due to the lack of recent magmatism and the deep crustal structure, which is between 42 and 47 km thick. [44]

2.2 Pannonian Basin

The Pannonian Basin lies within the convergence zone between the Eurasian and Nubian plates, where the ongoing subduction of oceanic and continental lithosphere led to the development of back-arc basins [47]. It is bordered by the Eastern and Southern Alps in the west, by the Dinarides in the south, by the Apuseni Mountains and the Southern Carpathians in the east, and by the Western and Eastern Carpathians in the north [48]. On the Romanian territory, the Pannonian basin is located in the northwestern part of the country, close to the Hungarian border[49]. The Apuseni Mountains create the boundary between the Pannonian and Transylvanian basins[50].

The basement in this area is made up of crystalline rocks, which belong to various tectonic cycles and the magmatic intrusions associated with them [48]. The sedimentary fill of the basin includes deposits from the Permian, Mesozoic, and Cenozoic eras [48]. Triassic formations lie directly on top of the basement, in the southern part of the Oradea - Satu Mare region (for the location of this region refer to Figure 1), and consist of conglomerates, sandstone and clay, with carbonate rocks in the upper part [51]. Jurassic formations are present in the same region as the Triassic, and consist mainly of terrigenous and carbonate deposits [51]. Lower Cretaceous deposits lie transgressively over the Jurassic and cover a larger surface area in the same region [51]. They contain carbonates and marly-calcareous sediments. The Upper Cretaceous lies over the previous series and directly over the basement, as it covers almost all the basin in a marly-sandstone facies [51]. Paleogene formations are found in the northern part overlapping the basement, and consist of shales, marls and sandstones [51]. The Neogenic cover lies transgressively over the older series and consists of Pannonia facies of Miocene and Pliocene formations [51]. The Miocene formations generally consist of terrigenous, evaporitic deposits, tuff, and tuffite [51]. Pliocene deposits include sandstone, sand, marls, and clays [51]. One area of interest, along with a cross section, are presented in Figure 4.

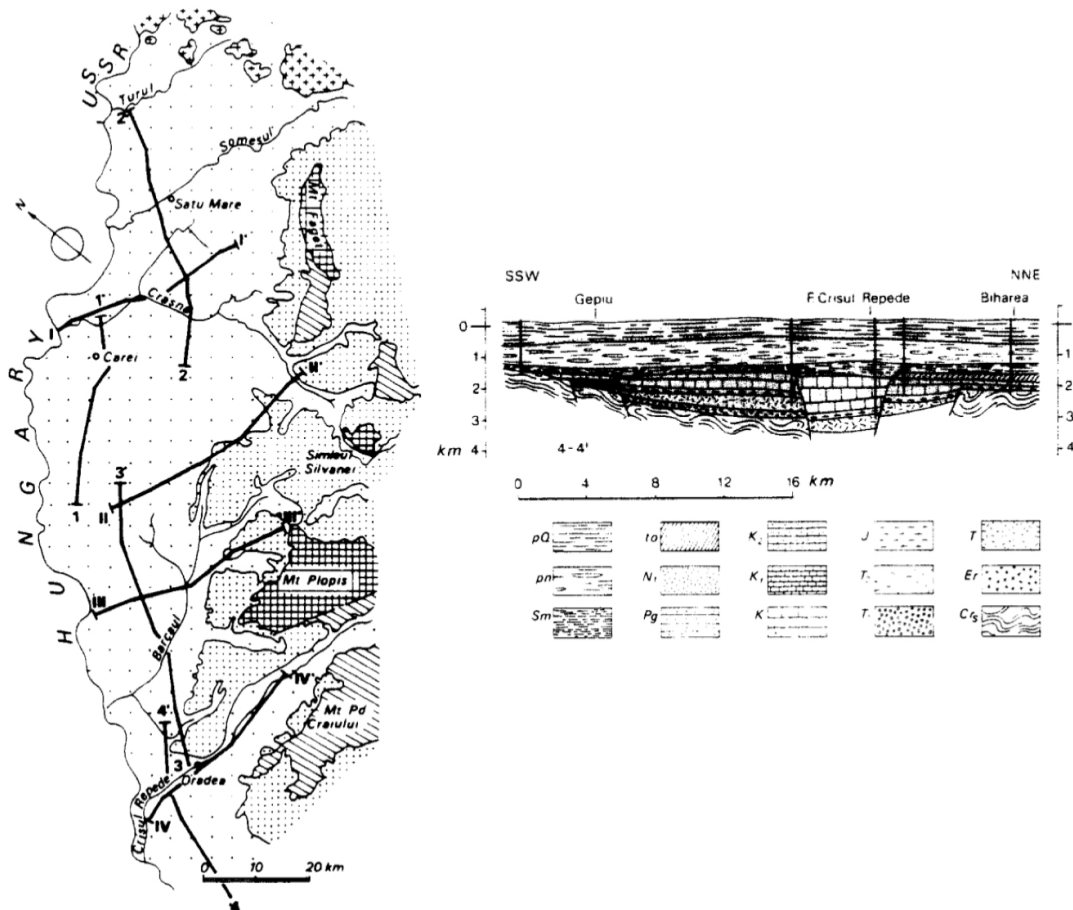


Figure 4: Sketch map of the Oradea-Satu Mare region (left) and one of the longitudinal geological cross-sections used for the Pannonian Basin (right), obtained from [51]. Er = magmatic rocks; Crs = crystalline basement; T = undifferentiated Triassic (T_1 = Lower Triassic, T_2 = Mid Triassic); J = Jurassic; K = undifferentiated Cretaceous (K_1 = Lower Cretaceous, K_2 = Upper Cretaceous); Pg = Paleogene; N = undifferentiated Miocene (To = Tortonian, Sm = Sarmatian); pn = Pannonian s.s.; pQ = Pontian-Quaternary.

2.3 Moesian Platform

The map displays the following features:

- Tectonic Units and Regions:** SOUTH CARPATHIANS, WEST MOESIA, EAST MOESIA, NORTH DOBROGEA OROGEN, CENTRAL DOBROGEA, SOUTH DOBROGEA, and BALKANS.
- Faults:** Timok Fault, Pericarpethian Fault, North Dobrogea Orogen PCF, IMF, AF, EF, and North Prebalkan Fault.
- Place Names:** Numerous locations are marked with triangles, including Chitili, Argetoaia, Rădări, Brazi, Capu Dealului, I Strehia, Făurești, Ștrăbulești, Ușurei, Căciulești, Opotasi, Corbu, Strâmbeni, Clărești, Dobreni, Sădănu, Chereshevo, Nikola Kozlevo, Vetroino, Belgun, Sablu, Văkino, Mangalia, 6082, Comana, Viroaga, Ograzhdze, Doulovo, Preslavci, 100Vlavin, Sălcia, Dierji, Leu, Băilești, Cetate, Gomotarci, Dărgodelci, Dărbani, Gârda Mare, Bănești, 62, 73, 24, 10, Slatina, Călineasa, 100Baly, Clărești, 35, 17, 11, 53 Tuzla, 6082, Mangalia, 6082, Văkino, Sablu, Belgun, Vetroino, Nikola Kozlevo, Ograzhdze, Doulovo, Preslavci, 100Vlavin, Sădănu, Dobreni, Clărești, Strâmbeni, Chureshi, Prosescu, Corbu, Ștrăbulești, Făurești, Ștrăbulești, Ușurei, Căciulești, Opotasi, Spineni, Hăbești, Bibesti, 6012 Mitrofanii, 62, 73, 24, 10, Slatina, Călineasa, 100Baly, Clărești, Dobreni, Sădănu, Chereshevo, Nikola Kozlevo, Vetroino, Belgun, Sablu, Văkino, Mangalia, 6082, Comana, Viroaga, Ograzhdze, Doulovo, Preslavci, 100Vlavin, Sălcia, Dierji, Leu, Băilești, Cetate, Gomotarci, Dărgodelci, Dărbani, Gârda Mare, Bănești, 62, 73, 24, 10, Slatina, Călineasa, 100Baly, Clărești, Dobreni, Sădănu, Dobreni, Clărești, Strâmbeni, Chureshi, Prosescu, Corbu, Ștrăbulești, Făurești, Ștrăbulești, Ușurei, Căciulești, Opotasi, Spineni, Hăbești, Bibesti, 6012 Mitrofanii.
- Geographic Coordinates:** The map is bounded by 22°E to 29°E longitude and 43°N to 46°N latitude.
- Scale:** A scale bar at the bottom indicates distances from 0 to 100 km.
- Inset Map:** A small inset map in the bottom right corner shows the location of the study area within the Balkan region, labeled 'B'.

The sedimentary fill of the platform generally reaches a thickness of around 10 km, except in the northeast area, where it exceeds 15 km, marking the thickest sedimentary sequence in Romania [55]. The stratigraphy of the western sector can be seen in Figure 6. Paleozoic formations consist of quartzitic sandstone, shale, limestone, dolomite, and evaporites [56]. The overlying Permian deposits include limestone, anhydrite, and salt, while the Triassic formations are composed mostly of carbonates and evaporites, with some magmatic intrusions [56]. Jurassic deposits consist mainly of limestone, dolomite, and shale, and the Cretaceous formation features carbonate and siliclastic rocks [56]. The Miocene comprises sandstones, marls, carbonates, and evaporites, while the Cenozoic cover concludes sedimentation with mainly sandstone [56].

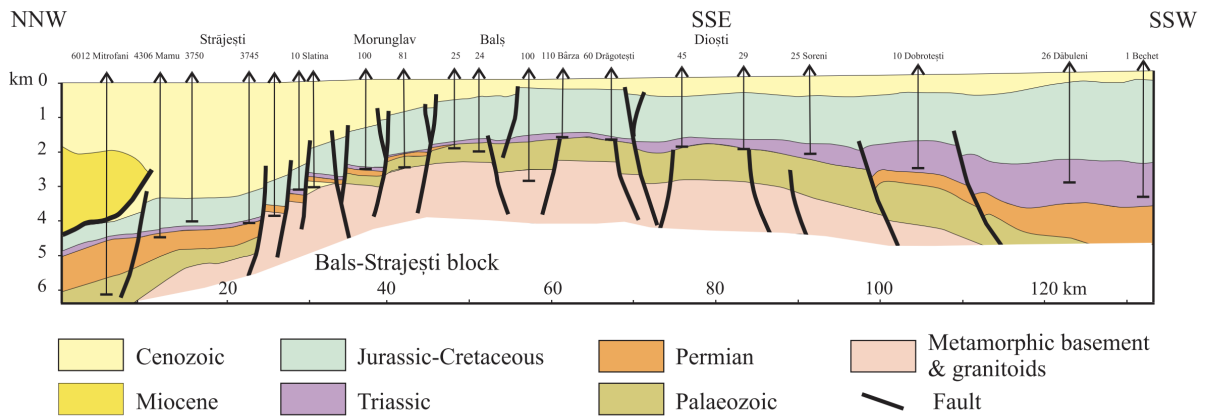


Figure 6: Geological cross-section in West Moesia. The approximate location can be seen in Figure 5, obtained from [53].

The heat flow values vary throughout the platform between 20 and 70 $\text{mW} \cdot \text{m}^{-2}$ [57]. The western sector presents a higher geothermal gradient, of 5-6 $^{\circ}\text{C} \cdot \text{km}^{-1}$, compared to 1.5 $^{\circ}\text{C} \cdot \text{km}^{-1}$ in the eastern sector [58]. The high heat flow is linked to the magmatic activity that took place between the Permian and Triassic, as well as the breakdown of radiogenic elements within the magmatic rocks, with deep faults acting as pathways for fluid circulation [58].

3 Methodology

In order to perform an assessment of geothermal potential, regions of elevated geothermal gradient have to be identified, along with estimates of heat that could theoretically be extracted from reservoir rocks. The methodology used to carry out this assessment is outlined in the following sections. The maps were generated using QGIS, which is a geographic information system that facilitates spatial processing, visualization, and interpretation of georeferenced data[59].

3.1 Geothermal Gradient

The heat flow map obtained from [60] was georeferenced on an OpenStreetMap standard base map to ensure spatial alignment. 20 wells investigated in the original study were digitized as point features in a multipoint shapefile layer, with their geothermal gradient values stored as attribute fields. The resulting point dataset was interpolated using Ordinary Kriging, which is a geostatistical method that estimates unknown values based on the spatial autocorrelation of the known data points [61]. To limit the output to the study area, a polygon shapefile of the national boundary was used to clip the interpolated surface.

3.2 Recoverable Heat

In order to assess the theoretical amount of heat that could be extracted from reservoir rocks, a reformulation of the USGS volumetric heat-in-place method was employed [62]. The recoverable heat was computed using [62]:

$$q_R = V \rho c_p (T_R - T_{ref}) \quad (1)$$

where q_R is the recoverable heat, V is the net volume of the reservoir, ρc_p is the volume-related specific heat capacity of the rock, T_R is the average temperature of the reservoir, and T_{ref} is the reference temperature, taken as 15 °C [62].

3.2.1 Volume Estimation

To apply this method, geological cross sections for each region were used as the basis to compute the volume of the layers. The cross sections presented in Figures 3 and 6 were used to compute the depth of the top and base of each layer, for the Transylvanian Basin and the Moesian Platform, respectively. For the Pannonian Basin, the cross sections provided in [51] were used as reference, as they represent the only extensive data available for this region. The longitudinal cross sections for the Oradea-Satu Mare region were cropped and merged together to form a continuous cross section for the area.

Due to the age and resolution of the original publication, the quality of the cross sections was limited in the Pannonian Basin, which made stratigraphic interpretation challenging. The lithological boundaries were often unclear and some symbols were faded, further reducing the precision in identifying individual formations. In many cases, it was not possible to determine whether a layer corresponded to a specific subgroup or represented a broader stratigraphic interval. As a result, units from the same epoch or period were grouped together and treated as a single layer in the analysis, to allow for a more reliable estimation of the depth values. The dataset corresponding to each area of interest is available in Appendix A.

The area of each layer was computed using a Python code, available in Appendix C. To minimize the uncertainty in the area approximation, the cross sections were divided into vertical increments of 250 m. For each increment, the code determined the average thickness of the layer, and calculated its corresponding area using trapezoidal integration along the horizontal extent. The resulting values are provided in Appendix B.

To compute the gross volume of the layers, a lateral extent of 10 km was used. For the Transylvanian Basin, this choice was supported by the available cross sections, which suggest a relatively even subsurface geometry. In the Oradea-Satu Mare region, the reservoir appears to exhibit a dipping geometry, making the 10 km extent a conservative choice to avoid volume overestimation. However, for the Arad-Timisoara region and the Moesian Platform, no additional cross sections were available to indicate how the subsurface extends laterally, therefore the 10 km were treated as a cautious default. To compute the net volumes, a net-to-gross ratio was estimated for each layer based on the lithological composition described in Section 2 and assuming equal proportions among the identified rock types. The resulting values are available in Appendix B.

3.2.2 Estimation of Reservoir Temperatures

Following the volume calculations, reservoir temperatures were calculated for each layer increment using the formula [63]:

$$T_r = T_{\text{ref}} + T_g \cdot d_{\text{avg}} \quad (2)$$

where T_g is the geothermal gradient in $^{\circ}\text{C} \cdot \text{km}^{-1}$, and d_{avg} is the average depth of the layer.

As the geothermal gradient map was created using a sparse set of data points, it might not be fully representative of detailed spatial variations. Therefore, one geothermal gradient was assigned to each region as a representative average, based on its proximity to the areas of interest and using the values reported in [60], namely $28^{\circ}\text{C} \cdot \text{km}^{-1}$ for the Transylvanian Basin, $35^{\circ}\text{C} \cdot \text{km}^{-1}$ for the Moesian Platform, $50.5^{\circ}\text{C} \cdot \text{km}^{-1}$ for the Oradea-Satu Mare region, and $45^{\circ}\text{C} \cdot \text{km}^{-1}$ for the Arad-Timisoara region.

3.2.3 Estimation of Recoverable Heat

The volume-related specific heat capacity was estimated using the values in [64], applying the same assumption of equal distribution of the various lithologies as for the net-to-gross ratio. This parameter, alongside the previously determined volume and temperature estimates, was then used to compute the recoverable heat for each vertical increment. The total heat was obtained by summing the values across all increments within each layer.

3.2.4 Map Creation

The cross sections were georeferenced and the profile of each layer was digitized as a line shapefile. To account for the lateral extent, a buffer geoprocessing tool was used to generate polygon layers, representative of the spatial footprint of each unit. The overlap between polygons was visually assessed and manually digitized into a new polygon layer for each region, with their corresponding values recorded as attribute fields. To enable consistent comparison between regions and ensure all cross sections were visualized on the same scale, the resulting

polygon layers were merged.

Although the data was sparse, an interpolation along the areas of interest was performed, to provide a broad approximation of spatial trends. Random points, spaced at 3 km intervals, were generated along the centerline of each polygon. The attribute fields of the underlying polygons were transferred to the points through a spatial join, in order to be representative of the values at each location. Ordinary Kriging was once more employed to interpolate continuous surfaces, which were clipped to the boundaries of each area of interest.

4 Results and Discussion

The following section presents the results of the study and their interpretation, beginning with an analysis of geothermal gradients, followed by the estimation of recoverable heat. The final part outlines the main limitation of the study and offers directions for future research.

4.1 Geothermal Gradient

The geothermal gradient represents a key parameter in assessing geothermal potential, as it determines how rapidly the temperature increases with depth and, consequently, the drilling depth required to reach exploitable resources. Shallower depths are more favorable for economic and technical feasibility, and therefore, high geothermal gradients are preferred for geothermal exploitation. Their distribution across Romania is shown in Figure 7.

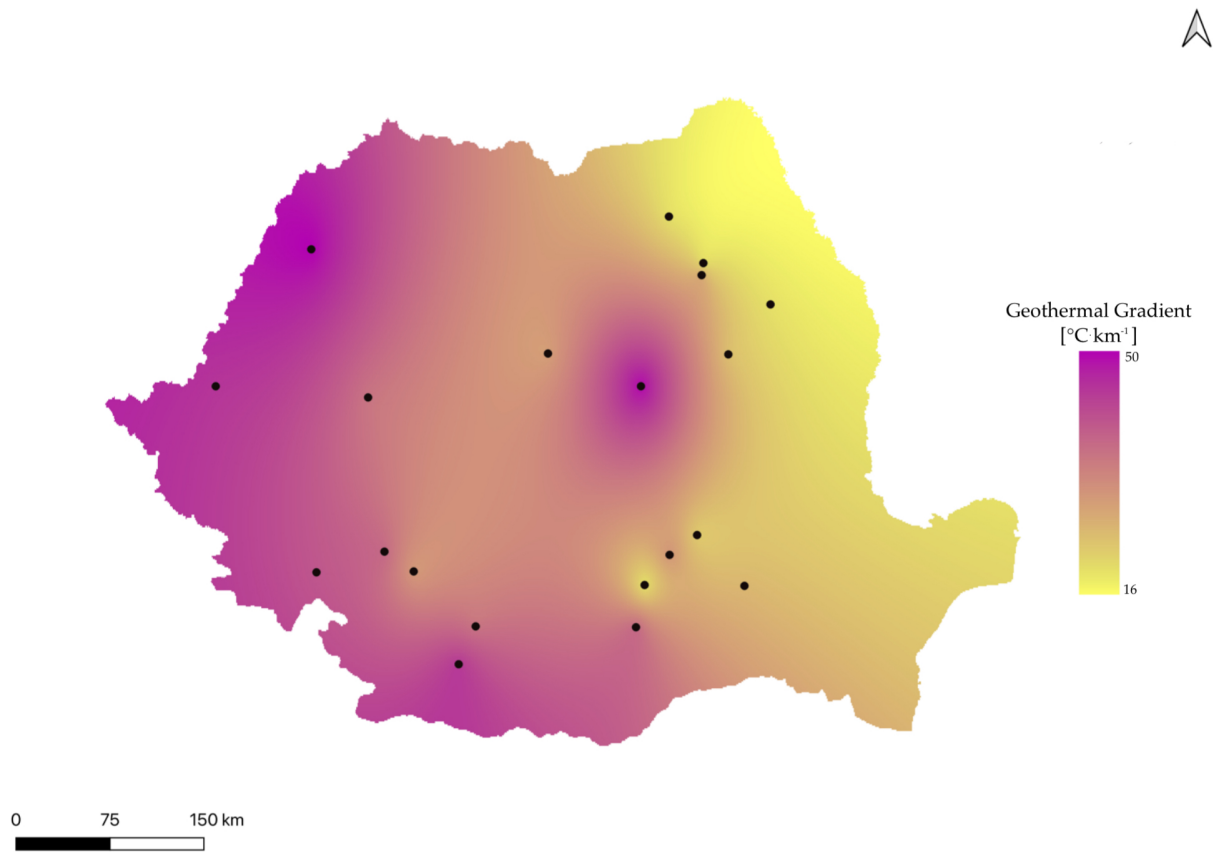


Figure 7: Geothermal gradient map of Romania. Black dots indicate the locations of the wells used to determine the geothermal gradients in [60].

A clear contrast in geothermal gradient values is observed throughout the country. The highest gradients, exceeding $45\text{ }^{\circ}\text{C} \cdot \text{km}^{-1}$, are found in the western regions, particularly in the Pannonian Basin. In comparison, the eastern part of the country exhibits the lowest gradients, ranging between 16 and $22\text{ }^{\circ}\text{C} \cdot \text{km}^{-1}$. Central Romania, which includes the Transylvanian Basin, is characterized by moderate gradients, with values ranging between 25 and $35\text{ }^{\circ}\text{C} \cdot \text{km}^{-1}$. The notable hotspot east of the basin stands out from the surrounding low-gradient zones and aligns with the location of more recent volcanic formations in the Eastern Carpathians [65]. In the south, the Moesian Platform shows internal variation, with its western sector presenting gradients between 22 and $45\text{ }^{\circ}\text{C} \cdot \text{km}^{-1}$, while the eastern sector exhibits ranges between 16 and

$22^{\circ}\text{C} \cdot \text{km}^{-1}$, consistent with patterns reported in literature [58]. It should be noted that the map was constructed using a limited data set, and while it provides a useful overview of regional trends, it is insufficient to capture detailed spatial variations, as further emphasized by the apparent minimal variability in some areas.

The spatial distribution of geothermal gradients broadly aligns with the current pattern of geothermal energy utilization presented in Table 2. Most operational wells are concentrated in the high-gradient areas of the Pannonian Basin, while areas such as the western sector of the Moesian Platform and the Transylvanian Basin show little to no utilization, despite their relatively elevated gradients, which indicate promising opportunities for further exploration. By contrast, the eastern sector of the Moesian Platform and the adjacent regions show the lowest geothermal gradients, which are consistent with the absence of known operational wells.

4.2 Recoverable Heat

The total recoverable heat estimated across the study area amounts to approximately 634 EJ. This estimate covers a total surface area of 5080 km^2 , distributed among the three main regions. The Transylvanian Basin accounts for around 171 EJ over an area of 1980 km^2 , while the Pannonian Basin contributes the largest share, with 280 EJ across 1760 km^2 . The Moesian Platform has an estimate of 183 EJ over 1340 km^2 . The spatial distribution of recoverable heat across these regions is illustrated in Figure 8.

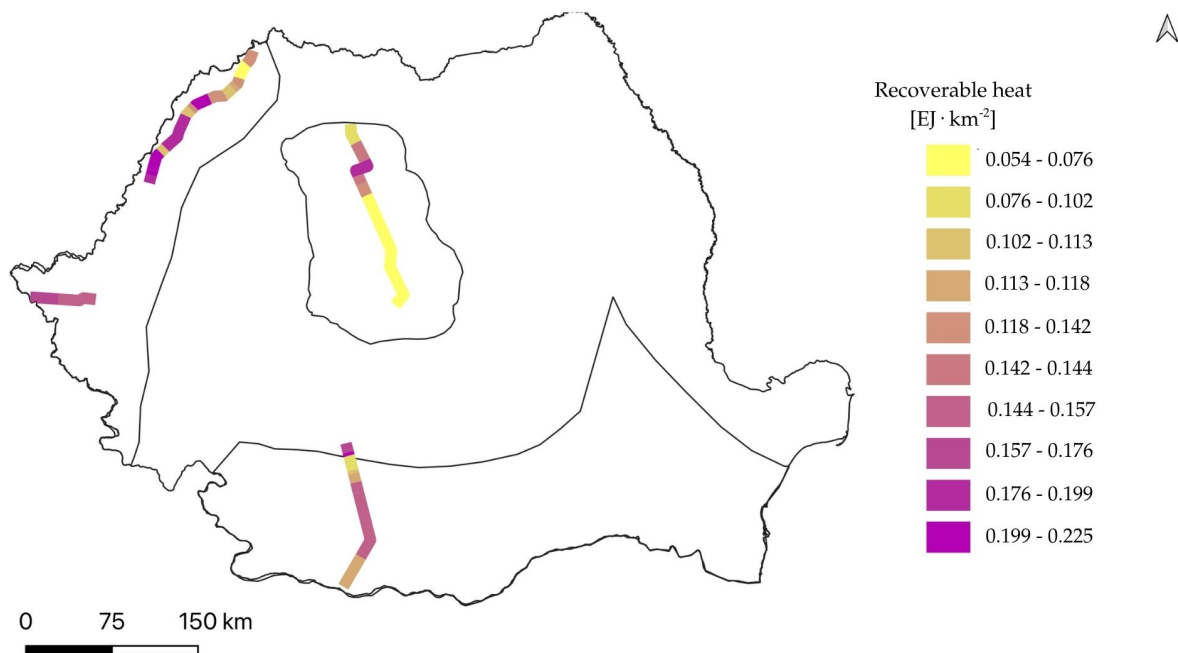


Figure 8: *Spatial distribution of recoverable heat density along the selected cross sections.*

To further visualize the heat-in-place distribution, an interpolation was performed using points extracted along the centerline of the four cross sections. The individual results of the interpolation are illustrated in Figure 9. Similarly to the geothermal gradient map, due to the sparse and uneven distribution of data points throughout each area, the interpolation does not provide a fully representative overview of each region. It fails to capture changes in subsurface geometry or local variations in geothermal gradient. Despite these limitations, the resulting maps offer a

preliminary indication of areas with elevated geothermal potential, and could serve as motivation for future studies to explore these regions using more detailed subsurface data and larger spatial coverage, especially considering the apparent untapped potential.

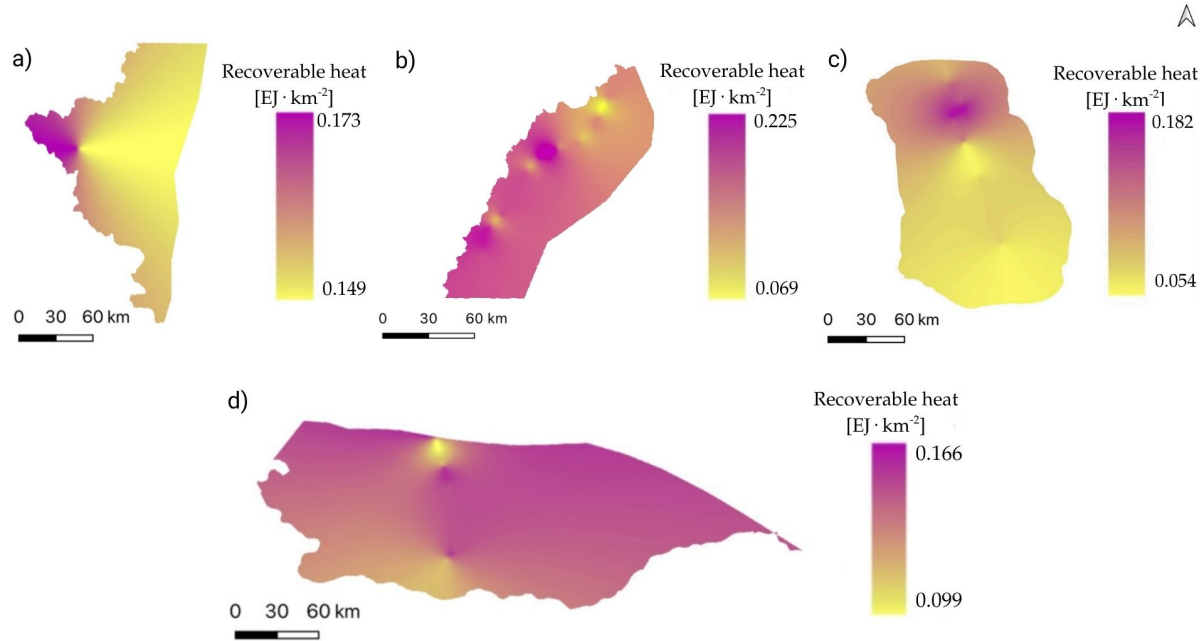


Figure 9: *Interpolated maps of recoverable heat density for: a) Oradea-Satu Mare region in the Pannonian Basin, b) Timisoara-Arad region in the Pannonian Basin, c) Transylvanian Basin and d) western sector of the Moesian Platform.*

Since only a fraction of the theoretical estimate of recoverable heat can be utilized effectively, a recovery factor was applied to estimate the technical potential. In the absence of site-specific data, a value of 1% was used, which is consistent with previous regional or global assessments[13]. The technical geothermal potential identified in this study is estimated at 0.634 EJ, over a system lifetime of 30 years [13], which corresponds to an annual average of 0.021 EJ. The total final energy demand for heating and cooling in Romania is approximately 0.580 EJ per year, of which 0.280 EJ is attributed to the residential sector, as of 2015 [28]. Although the estimate of the current study is based on only around 2% of the country's surface area and constrained by the limited subsurface data availability, the result is promising. If similar geothermal conditions can be identified across broader regions, geothermal energy could make a meaningful contribution to meeting Romania's long term heating demand.

The variation in recoverable heat between regions is primarily driven by differences in geothermal gradient. All layers were analyzed up to 3.75 km, which made the maximum temperatures play a key factor in the estimates. The Transylvanian Basin, with the lowest gradient of $28^{\circ}\text{C} \cdot \text{km}^{-1}$, reached a maximum temperature of around 116°C . In contrast, the Moesian Platform had a gradient of $35^{\circ}\text{C} \cdot \text{km}^{-1}$, resulting in a maximum temperature of 141°C . In the Pannonian Basin, geothermal gradients were significantly higher, reaching up to $50.5^{\circ}\text{C} \cdot \text{km}^{-1}$ in the Oradea-Satu Mare area, with corresponding temperatures of up to 200°C . These values are nearly double the maximum temperatures reached in the Transylvanian Basin, which further highlights the thermal advantage of the western region.

The geothermal potential of the Transylvanian Basin may have been underestimated due to the exclusion of key geological factors. Although salt structures were present in the Transylvanian Basin, they were not considered in this study. Rock salt exhibits significantly higher thermal conductivity at shallow depths compared to surrounding sedimentary rocks, which can result in localized increases in geothermal gradients above or around salt structures [66]. Similarly, volcanic areas located along the basin margins were excluded, and their inclusion in future studies could highlight additional zones of high geothermal potential [14].

In contrast, the Pannonian Basin may have been subject to overestimation of resource potential, stemming from the limitations in resolution and clarity of the available stratigraphic data. The cross sections were based on a publication from 1981, with faded symbols and occasional unclear boundaries, which required grouping of multiple units into broader intervals to ensure consistent depth estimation. While this workaround enabled a complete analysis, it may have led to misidentified layers, overestimated thicknesses, and consequently higher heat-in-place values in some areas.

The main source of uncertainty in this assessment is related to the estimation of the reservoir area. The depths to the top and base of each geological layer were determined visually from geological cross sections, which varied in resolution and quality. As a result, the interpretation may contain inaccuracies, which could have led to an overestimation of volumes, and therefore recoverable heat. Additionally, the exact lithological composition of each layer was unknown, which may have introduced inaccuracies in the estimated net-to-gross ratios and the specific heat capacity values used. Furthermore, due to the limited data availability regarding geothermal gradients, a single representative was assigned to each cross section, which made the resulting temperature estimates uniform along their horizontal profile and potentially less accurate in capturing local variations, such as those around the salt domes in the Transylvanian Basin.

A European-scale assessment has estimated the total geothermal resource base in Romania to approximately $2.4 \cdot 10^5$ EJ, distributed across an area of roughly 240000 km² [67]. The results of the present study account for only 0.2% of this total recoverable heat, and cover nearly 2% of the country's surface area. The average heat-in-place density in the European study is approximately $1000 \text{ PJ} \cdot \text{km}^{-2}$, whereas the current analysis indicates a lower value of about $124 \text{ PJ} \cdot \text{km}^{-2}$. The difference can be primarily attributed to the methodological differences, as Vieira et al. [67] do not account for geological variability when estimating reservoir volume, and rely on grid cell area and a uniform thickness applied throughout the entire territory only. Additionally, a shallower maximum depth was considered in this study. A maximum depth of 3.75 km was chosen, while the European assessment considered depths of up to 6km, which encompass significantly higher temperature intervals. While this approach increases theoretical heat-in-place values, it risks overestimating the feasible geothermal resources. By incorporating geological constraints, the present study provides a potentially more realistic estimate of Romania's average geothermal resource potential.

Using the same approach as the European assessment, Trumphy et al. [68] have estimated an average of $660 \text{ PJ} \cdot \text{km}^{-2}$ of recoverable heat for the South of Italy. The higher order of magnitude can once again be attributed to the methodological differences, particularly the simplified volume estimation, which most likely led to the overestimation of resources.

Furthermore, in the Netherlands, the recoverable heat reaches up to $0.027 \text{ EJ} \cdot \text{km}^{-2}$ [69, 70], while in the Croatian part of the Pannonian Basin it can amount to as much as $1.4 \text{ EJ} \cdot \text{km}^{-2}$ in isolated locations [71]. The present study, however, estimates a maximum of $0.225 \text{ EJ} \cdot \text{km}^{-2}$. While all three studies consider geological layering, the Dutch and Croatian studies rely on doublet-based modeling that incorporates system specific assumptions, such as fluid extraction or reinjection. As a result, they focus on specific reservoirs only, and do not evaluate the entire rock column, as in the current study. The discrepancy in estimates can also be explained by the differences in geothermal gradients. The Dutch study applies a geothermal gradient of $30 \text{ }^{\circ}\text{C} \cdot \text{km}^{-1}$, while the Croatian study uses a maximum gradient of $72 \text{ }^{\circ}\text{C} \cdot \text{km}^{-1}$, which is almost $22 \text{ }^{\circ}\text{C} \cdot \text{km}^{-1}$ higher than the gradient associated with the maximum recoverable heat presented in this study. Moreover, the Dutch analysis includes a recovery factor when estimating the potential recoverable heat.

4.3 Future Outlooks

The main limitation of this study was the lack of available subsurface data. Information from geothermal, oil, and gas wells, such as temperature measurements or lithological descriptions, collected by the National Agency of Mineral Resources, are not publicly available. Because of this, the analysis relied on geological cross sections, scarcely available in literature, which restricted the investigation to a limited part of the country. Future studies would benefit from better access to well data, particularly from existing exploration and production wells. Although collaboration with national institutions or companies holding this information was attempted, access could not be obtained for the purpose of this study. Future efforts to acquire such data could help expand the geographic scope and improve the accuracy of the results.

The lack of detailed subsurface data also required the use of generalized reservoir parameters, such as specific heat capacity, net-to-gross ratios, and geothermal gradients, that were applied uniformly across all regions. These simplifications introduce uncertainty, as such properties vary with lithology, depth, or geological conditions. Future research should integrate detailed lithological and stratigraphic data, as well as a broader set of geothermal gradients, to assign more realistic, location specific reservoir properties.

With improved data availability, future assessments could also transition from 2D cross-sectional interpretations to more advanced 3D geological modeling. This would allow for better representation of subsurface variability, reduce the reliance on interpolation, and improve accuracy of volume and temperature estimates. Developing a centralized geothermal data platform and encouraging institutional collaboration would be critical steps toward enabling these improvements.

Despite the limitations of the current analysis, the results indicate that Romania holds considerable geothermal potential, even across a small and data limited portion of its territory. This suggests that future investigations could uncover substantial untapped resources, and expanding this line of research would be a detrimental step toward reducing fossil fuel dependency and meeting national heating demands through sustainable means.

5 Conclusions

Romania has significant geothermal resources, yet their overall utilization remains limited, with most applications being found in the western part of the country. The scope of this study was to assess the geothermal resource potential of Romania, by constructing a geothermal gradient map and applying a volumetric heat-in-place approach to estimate the theoretical maximum amount of heat that could be extracted from reservoir rocks. The analysis focused on the three main sedimentary basins in the country, namely the Pannonian Basin, the Transylvanian Basin, and the Moesian Platform, as sedimentary basins are known to have favorable conditions for geothermal development.

The geothermal gradient map showed a clear contrast across Romania, with the Pannonian Basin exhibiting the highest values, exceeding $45\text{ }^{\circ}\text{C} \cdot \text{km}^{-1}$. The spatial distribution of geothermal gradients broadly aligns with the current geothermal applications, but highlights high potential areas with little to no utilization in the Moesian Platform and the Transylvanian Basin. Since the map was created using a relatively low number of gradients, it provides a general approximation of regional trends, and future studies should include a broader set of data points to capture more detailed spatial variations.

As for recoverable heat, the total estimate was approximately 634 EJ, across a surface area of 5080 km^2 . The Pannonian Basin had the highest contribution with 280 EJ across 1760 km^2 , followed by the Moesian Platform at 183 EJ over 1340 km^2 . The Transylvanian Basin accounted for around 171 EJ over an area of 1980 km^2 . The variability in values were primarily attributed to the variation in geothermal gradients across the three regions. Overestimation of the potential could be attributed to the generalization and uniform application of reservoir properties, such as geothermal gradients, specific heat capacities, and net-to-gross ratios, due to the absence of site specific data. Additionally, the quality and resolution of the geological cross sections, combined with their visual interpretation, could have contributed to the overestimation of layer areas, and consequently the recoverable heat estimate. Since the main limitation of the study was the limited data availability, future research should focus on acquiring data from geothermal, oil, or gas wells, in order to expand the geographic scope of the assessment and increase the accuracy of the results. Despite the limited spatial coverage and lack of site-specific data, the study identified an annual technical potential of 0.021 EJ, which represents roughly 4% of Romania's yearly heating and cooling demand.

In comparison with a European assessment, which reported an average of $1000\text{ PJ} \cdot \text{km}^{-2}$, the present study offered a more grounded estimate of $124\text{ PJ} \cdot \text{km}^{-2}$, by incorporating geological constraints. While the European approach relied on uniform reservoir thicknesses and overlooked geological variability, the current analysis considered the stratigraphy, lithology, and regional depth limitations of the formations, offering a more realistic result.

These promising results, obtained from only around 2% of the country's surface area, indicate that Romania holds considerable untapped geothermal resources. Expanding this line of research could play a key role in reducing fossil fuel dependency and supporting the long term heating demands of the country.

Bibliography

- [1] C. I. Igwe, “Geothermal energy: A review,” *International Journal of Engineering Research and Technology (IJERT)*, vol. 10, no. 3, pp. 655–664, 2021.
- [2] A. Manzella, “Geothermal energy,” *EPJ Web of Conferences*, vol. 148, p. 00012, 2017.
- [3] T. Lay, J. W. Hernlund, and B. A. Buffett, “Core–mantle boundary heat flow,” *Nature Geoscience*, vol. 1, no. 1, pp. 25–32, 2008.
- [4] National Research Council (US) Committee on the Biological Effects of Ionizing Radiations, *Health Risks of Radon and Other Internally Deposited Alpha-Emitters: BEIR IV*. Washington, DC: National Academies Press, 1988.
- [5] J. R. Muir, A. J. Van Horn, and J. W. Hill, “Geothermal energy as a premium power source – resilient continuous power,” in *GRC Transactions*, vol. 46, 2022.
- [6] C. I. Igwe, “Geothermal energy: A review,” *Nnamdi Azikiwe University Awka*, n.d.
- [7] J. Finger and D. Blankenship, “Handbook of best practices for geothermal drilling,” Tech. Rep. SAND2010-6048, Sandia National Laboratories, 2010. Prepared for the International Energy Agency, Geothermal Implementing Agreement.
- [8] TNO and EGEC, “Prospective study on the geothermal electricity potential in the eu in 2020/2030/2050,” tech. rep., GEOELEC Project, Intelligent Energy – Europe (IEE), Brussels, Belgium, 2013. Deliverable n° 2.5, November 2013.
- [9] Ábel Markó, J. Mádl-Szőnyi, and M. Brehme, “Injection related issues of a doublet system in a sandstone aquifer – a generalized concept to understand and avoid problem sources in geothermal systems,” *Geothermics*, vol. 97, p. 102234, 2021.
- [10] G. Axelsson, E. Juliusson, H. Franzson, H. Einarsson, H. Ármannsson, B. Thórhallsson, *et al.*, “Geothermal well performance testing in iceland,” *Energies*, vol. 7, no. 7, pp. 4397–4427, 2014.
- [11] A. C. Gringarten, “Reservoir lifetime and heat recovery factor in geothermal aquifers used for urban heating,” *Pageoph (Pure and Applied Geophysics)*, vol. 117, pp. 297–308, 1978.
- [12] J. Clauser, M. Bär, T. Kohl, T. Hoppe, S. Backers, K. Reinicke, B. Valladares, K. Krüger, S. Held, and J. J. Ritter, “A study on the lifetime of a two-well enhanced geothermal system,” *Geothermics*, vol. 91, p. 102024, 2021.
- [13] J. Limberger, T. Boxem, M. Pluymaekers, D. Bruhn, A. Manzella, P. Calcagno, F. Beekman, S. Cloetingh, and J.-D. van Wees, “Geothermal energy in deep aquifers: A global assessment of the resource base for direct heat utilization,” *Renewable and Sustainable Energy Reviews*, vol. 82, pp. 961–975, 2018.
- [14] J. Twidell and T. Weir, *Renewable Energy Resources*. Abingdon, UK: Taylor & Francis, 2nd ed., 2006.
- [15] C. Augustine, J. W. Tester, B. Anderson, S. Petty, and B. Livesay, “A comparison of geothermal with oil and gas well drilling costs,” in *Proceedings, Thirty-First Workshop on Geothermal Reservoir Engineering*, (Stanford, California), Stanford University, 2006. SGP-TR-179.

-
- [16] M. A. Grant and P. F. Bixley, *Geothermal Reservoir Engineering*. Amsterdam, Boston, Heidelberg, London, New York, Oxford, Paris, San Diego, San Francisco, Singapore, Sydney, Tokyo: Academic Press, 2nd ed., 2011.
- [17] H. Aydin and C. Temizel, “Characterization of geothermal reservoirs,” in *Proceedings, 47th Workshop on Geothermal Reservoir Engineering*, no. SGP-TR-223, (Stanford University, Stanford, California, February 7–9), Stanford University, 2022.
- [18] M. Hanano, “Contribution of fractures to formation and production of geothermal resources,” *Renewable and Sustainable Energy Reviews*, vol. 8, no. 3, pp. 223–236, 2004.
- [19] Z. Xie, D. Han, J. Li, and K. Li, “A state-of-the-art review of hydraulic fracturing in geothermal systems,” *Sustainability*, vol. 16, no. 24, p. 11087, 2024.
- [20] R. Schultz, “Hydraulic fracturing-induced seismicity,” *Reviews of Geophysics*, vol. 58, no. 3, p. e2019RG000695, 2020.
- [21] M. Schmitt, C. P. Fernandes, J. A. da Cunha Neto, F. G. Wolf, and V. S. dos Santos, “Characterization of pore systems in seal rocks using nitrogen gas adsorption combined with mercury injection capillary pressure techniques,” *Marine and Petroleum Geology*, vol. 39, pp. 138–149, 2013.
- [22] N. Aksoy, C. Şimşek, and O. Gunduz, “Groundwater contamination mechanism in a geothermal field: A case study of balcova, turkey,” *Journal of Contaminant Hydrology*, vol. 103, no. 1–2, pp. 13–28, 2009.
- [23] A. Leins, D. Bregnard, A. Vieth-Hillebrand, P. Junier, and S. Regenspurg, “Dissolved organic compounds in geothermal fluids used for energy production: a review,” *Geothermal Energy*, vol. 10, no. 9, 2022.
- [24] S. Regenspurg, M. Alawi, G. Blöcher, M. Börger, S. Kranz, B. Norden, A. Saadat, T. Scheytt, L. Virchow, and A. Vieth-Hillebrand, “Impact of drilling mud on chemistry and microbiology of an upper triassic groundwater after drilling and testing an exploration well for aquifer thermal energy storage in berlin (germany),” *Environmental Earth Sciences*, vol. 77, no. 516, 2018.
- [25] M. Rosca, C. Karytsas, and D. Mendrinou, “Low enthalpy geothermal power generation in romania,” in *Proceedings of a Conference*, 2010.
- [26] C. Bendea, C. Antal, and M. Roşca, “Geothermal energy in romania: Country update 2010–2014,” in *Proceedings World Geothermal Congress 2015*, (Melbourne, Australia), pp. 1–9, International Geothermal Association, April 2015.
- [27] M. Rosca, C. Antal, and C. Bendea, “Geothermal energy in romania: Country update 2005–2009,” *Proceedings of the World Geothermal Congress*, 2010.
- [28] Heat Roadmap Europe Project Team, “2015 final heating & cooling demand in romania – country presentation.” PowerPoint presentation, October 2017. Presented in October 2017 under the EU Horizon 2020 programme, grant agreement no. 695989.
- [29] M. Rosca and M. Antics, “Current status of geothermal energy utilization in romania,” in *International Geothermal Days POLAND 2004*, (Zakopane, Poland), 2004.

-
- [30] Primăria Municipiului Beiuș, “Beiuș, oraș geotermal, orașul ecologic,” 2024. Accessed: 2025-04-29.
 - [31] C. Antal, F. Popa, M. Mos, D. Tigan, B. Popa, and V. Muresan, “Advanced concepts and solutions for geothermal heating applied in oradea, romania,” in *IOP Conference Series: Materials Science and Engineering*, vol. 163, p. 012029, 2017.
 - [32] A. Blaga, M. Rosca, C. Karytsas, and D. Mendrinou, “Possible geothermal district heating in sanmartin, romania,” in *Proceedings of a Conference*, 2005.
 - [33] S. Dimitriu, A.-M. Bianchi, and F. Băltărețu, “The up-to-date heat pump–combined heat and power solution for the complete utilization of the low enthalpy geothermal water potential,” *International Journal of Energy and Environmental Engineering*, vol. 8, pp. 189–196, 2017.
 - [34] I. Sarbu, M. Mirza, and D. Muntean, “Integration of renewable energy sources into low-temperature district heating systems: A review,” *Energies*, vol. 15, no. 18, p. 6523, 2022.
 - [35] R. Gavriluic, M. Rosca, C. Bendea, C. Antal, and D. Cucueteau, “Geothermal energy in romania - country update 2015–2019,” in *Proceedings of the World Geothermal Congress 2020+1*, (Reykjavik, Iceland), 2021. Available via: <https://www.geothermal-energy.org/pdf/WGC/papers/WGC2020/02071.pdf>.
 - [36] R. C. Selley and S. A. Sonnenberg, *Elements of Petroleum Geology*. Academic Press, 3rd ed., 2015.
 - [37] T. M. Letcher, ed., *Comprehensive Renewable Energy*. Elsevier, 2nd ed., 2022.
 - [38] D. T. Birdsell, B. M. Adams, P. Deb, J. D. Ogland-Hand, J. M. Bielicki, M. R. Fleming, and M. O. Saar, “Analytical solutions to evaluate the geothermal energy generation potential from sedimentary-basin reservoirs,” *Geothermics*, vol. 116, p. 102843, 2024.
 - [39] C. M. Bethke, S. P. Altaner, W. J. Harrison, and S. Upson, “Supercomputer analysis of sedimentary basins,” *Science*, vol. 239, no. 4837, pp. 261–267, 1988.
 - [40] L. Rybach, “Geothermal potential of sedimentary basins, especially of the swiss molasse basin,” *Földtani Közlöny (Hungarian Geological Society)*, vol. 149, no. 4, pp. 401–414, 2019.
 - [41] J. Boggs, Sam, *Principles of Sedimentology and Stratigraphy*. PEARSON Prentice Hall, fourth ed., 2006.
 - [42] S. Filipescu, L. Silye, and C. Krézsek, “Stratigraphic overview of the neogene transylvanian basin, romania,” *Geological Society, London, Special Publications*, vol. 554, Oct 2024.
 - [43] S. M. Schmid, D. Bernoulli, B. Fügenschuh, L. Matenco, S. Schefer, R. Schuster, M. Tischer, and K. Ustaszewski, “The alpine-carpathian-dinaridic orogenic system: correlation and evolution of tectonic units,” *Swiss Journal of Geosciences*, vol. 101, no. 1, pp. 139–183, 2008.
 - [44] . A. Daniel Ciulavu, 1 Corneliu Dinu, “Neogene kinematics of the transylvanian basin (romania),” *AAPG Bulletin*, vol. 84, 2000.

-
- [45] B. M. Popescu, "Romania's petroleum systems and their remaining potential," *Petroleum Geoscience*, vol. 1, p. 337–350, Nov 1995.
- [46] M. S. Tiliță, *Evolution of the Transylvanian Basin: Inferences from Seismic Interpretation and Numerical Modelling*. Phd thesis, Utrecht University, 2015. Utrecht Studies in Earth Sciences, Volume 89.
- [47] F. Horváth, B. Musitz, A. Balázs, A. Végh, A. Uhrin, A. Nádor, B. Koroknai, N. Pap, T. Tóth, and G. Wörkum, "Evolution of the pannonian basin and its geothermal resources," *Geothermics*, vol. 53, pp. 328–352, 2015.
- [48] I. Panea and V. Mocanu, "Geophysical analysis of major geothermal anomalies in romania," *Pure and Applied Geophysics*, vol. 174, no. 9, pp. 4153–4169, 2017.
- [49] C. A. Roba, D. Niță, C. Cosma, V. Codrea, and Olah, "Correlations between radium and radon occurrence and hydrogeochemical features for various geothermal aquifers in northwestern romania," *Geothermics*, vol. 42, pp. 32–46, 2012.
- [50] D. Ciulavu, C. Dinu, and S. A. P. L. Cloetingh, "Late cenozoic tectonic evolution of the transylvanian basin and northeastern part of the pannonian basin: Constraints from seismic profiling and numerical modelling," *Stephan Mueller Special Publication Series*, vol. 3, pp. 105–120, 2002.
- [51] A. Țențu, T. Constantinescu, F. Davidescu, S. Nuțu, P. Noto, and P. Squarci, "Research on the thermal waters of the western plain of romania," *Geothermics*, vol. 10, no. 1, pp. 1–28, 1981.
- [52] R. S. Huismans, Y. Y. Podladchikov, and S. A. P. L. Cloetingh, "Dynamic modelling of the transition from passive to active rifting, application to the pannonian basin," *Tectonics*, vol. 20, no. 6, pp. 1021–1039, 2001.
- [53] A. Seghedi, M. Vaida, M. Iordan, and J. Verniers, "Paleozoic evolution of the romanian part of the moesian platform: An overview," *Geologica Belgica*, vol. 8, no. 4, pp. 99–120, 2005.
- [54] V. Raileanu, D. Tataru, and B. Grecu, "Crustal models in romania – i. moesian platform," *Romanian Reports in Physics*, vol. 64, no. 2, pp. 539–554, 2012.
- [55] N. Anastasiu and D.-R. Roban, "Post-depositional evolution of the carbonate reservoir systems of the moesian platform, romania," *Search and Discovery*, no. 50174, 2009. Adapted from extended abstract prepared for AAPG International Conference and Exhibition, Cape Town, South Africa, October 26–29, 2008.
- [56] M. J. Pawlewicz, T. Klett, and R. R. Charpentier, *Total Petroleum Systems of the Carpathian–Balkan Basin Province*, vol. 2204–F of *U.S. Geological Survey Bulletin*. U.S. Department of the Interior, U.S. Geological Survey, 2007.
- [57] C. Demetrescu and M. Andreescu, "On the thermal regime of some tectonic units in a continental collision environment in romania," *Tectonophysics*, vol. 230, no. 3–4, pp. 265–276, 1994.

- [58] M. Andreescu, D. Burst, C. Demetrescu, M. Ene, and G. Polonic, “On the geothermal regime of the moesian platform and getic depression,” *Tectonophysics*, vol. 164, pp. 281–286, 1989. In: V. Čermák, L. Rybach and E.R. Decker (Editors), *Heat Flow and Lithosphere Structure*.
- [59] QGIS.org, “QGIS Geographic Information System,” 2024.
- [60] S. Veliciu, M. Cristian, D. Paraschiv, and M. Visarion, “Preliminary data of heat flow distribution in romania,” *Geothermics*, vol. 6, no. 1–2, pp. 95–98, 1977.
- [61] H. Wackernagel, “Ordinary kriging,” in *Multivariate Geostatistics*, pp. 74–81, Berlin, Heidelberg: Springer, 1995.
- [62] S. K. Garg and J. Combs, “A reformulation of usgs volumetric “heat in place” resource estimation method,” *Geothermics*, vol. 55, pp. 150–158, 2015.
- [63] A. Satter and G. M. Iqbal, *Reservoir Engineering: The Fundamentals, Simulation, and Management of Conventional and Unconventional Recoveries*. Amsterdam: Gulf Professional Publishing / Elsevier, 2015.
- [64] Verein Deutscher Ingenieure (VDI), Düsseldorf, Germany, *VDI 4640 Blatt 1: Thermische Nutzung des Untergrundes – Grundlagen, Genehmigungen, Umweltaspekte*, 2010. Issue: German/English; The German version shall be taken as authoritative.
- [65] Z. Pécskay, J. Lexa, A. Szakács, I. Seghedi, K. Balogh, V. Konečný, T. Zelenka, M. Kovács, T. Póka, A. Fülöp, E. Márton, C. Panaiotu, and V. Cvetković, “Geochronology of neogene magmatism in the carpathian arc and intra-carpathian area,” *Geologica Carpathica*, vol. 57, pp. 511–530, December 2006.
- [66] J. Raymond, H. Langevin, F.-A. Comeau, and M. Malo, “Temperature dependence of rock salt thermal conductivity: Implications for geothermal exploration,” *Renewable Energy*, vol. 184, pp. 26–35, 2022. Available online 23 November 2021.
- [67] F. P. Vieira, S. N. P. Guimarães, J. L. d. S. Gomes, and V. M. Hamza, “Geothermal resources of european continent: A regional assessment,” *International Journal of Terrestrial Heat Flow and Applied Geothermics*, vol. 6, no. 1, pp. 11–18, 2023.
- [68] E. Trumpy, S. Botteghi, F. Caiozzi, A. Donato, G. Gola, D. Montanari, M. Pluymaekers, A. Santilano, J. van Wees, and A. Manzella, “Geothermal potential assessment for a low carbon strategy: A new systematic approach applied in southern italy,” *Energy*, vol. 103, pp. 167–181, 2016.
- [69] J.-D. van Wees, A. Kronimus, M. van Putten, M. Pluymaekers, H. Mijnlief, P. van Hooff, A. Obdam, and L. Kramers, “Geothermal aquifer performance assessment for direct heat production – methodology and application to rotliend aquifers,” *Netherlands Journal of Geosciences - Geologie en Mijnbouw*, vol. 91, no. 4, pp. 651–665, 2012.
- [70] L. Kramers, J.-D. van Wees, M. Pluymaekers, A. Kronimus, and T. Boxem, “Direct heat resource assessment and subsurface information systems for geothermal aquifers; the dutch perspective,” *Netherlands Journal of Geosciences - Geologie en Mijnbouw*, vol. 91, no. 4, pp. 637–649, 2012.

-
- [71] M. Tuschl and T. Kurevija, “Defining heat in place for the discovered geothermal brine reservoirs in the croatian part of pannonian basin,” *Water*, vol. 15, no. 6, p. 1237, 2023.

Appendices

A Raw Data

The raw data from the investigated cross sections is available in the following google drive: [Raw Data](#)

B Area and Volume Calculations

The regional areas and volumes for each increment are available in the following google drive: [Areas and Volumes](#)

C Python Source Code

The Google Colaboratory notebook can be accessed through the following link: [Area Code](#)